Interfaces and Free Boundaries **10** (2008), 399–421

Convergent and conservative schemes for nonclassical solutions based on kinetic relations. I

BENJAMIN BOUTIN, CHRISTOPHE CHALONS,
FRÉDÉRIC LAGOUTIÈRE AND PHILIPPE G. LEFLOCH
Laboratoire Jacques-Louis Lions & Centre National de la Recherche Scientifique, Université Pierre et Marie Curie (Paris 6), 4 Place Jussieu, 75252 Paris, France

[Received 10 July 2007 and in revised form 23 January 2008]

We propose a new numerical approach to computing nonclassical solutions to hyperbolic conservation laws. The class of finite difference schemes presented here is fully conservative and keeps nonclassical shock waves as sharp interfaces, unlike standard finite difference schemes. The main challenge is to achieve, at the discretization level, a consistency property with respect to a prescribed kinetic relation. The latter is required for the selection of physically meaningful nonclassical shocks. Our method is based on a reconstruction technique performed in each computational cell that may contain a nonclassical shock. To validate this approach, we establish several consistency and stability properties, and we perform careful numerical experiments. The convergence of the algorithm toward the physically meaningful solutions selected by a kinetic relation is demonstrated numerically for several test cases, including concave-convex as well as convex-concave flux functions.

1. Introduction

State of the art

We are interested here in the issue of numerically computing *nonclassical* solutions (containing undercompressive shocks) to nonlinear hyperbolic conservation laws. Nonclassical solutions have the distinctive feature of being dynamically driven by small-scale effects such as diffusion, dispersion, and other high-order phenomena. Their selection requires an additional jump relation, called a kinetic relation, and introduced in the context of phase transition dynamics by Slemrod [35, 36, 13], Truskinovsky [37, 38], Abeyaratne and Knowles [1, 2], LeFloch [23], and Shearer [33, 34], and developed in the more general context of nonlinear hyperbolic systems of conservation laws by LeFloch and collaborators [15]–[17], [3]–[5], [28]–[30], and [27]. See [24] for a review.

From pioneering work by Hayes and LeFloch [16] it is now recognized that standard finite difference schemes do not converge to nonclassical solutions selected by the prescribed kinetic function. In fact, kinetic functions can be associated not only with continuous models, but with the finite difference schemes themselves. Achieving a good agreement between the continuous and the numerical kinetic functions has been found to be very challenging. For recent work in this direction see [25].

Other affiliations of the first author: DEN/DANS/DM2S/ SFME/LETR CEA-Saclay, 91191 Gif-sur-Yvette, France, and of the second and third authors: Université Paris Diderot (Paris 7), 75251 Paris Cedex 05.
E-mails: Boutin@ann.jussieu.fr, Chalons@math.jussieu.fr, Lagoutie@math.jussieu.fr, LeFloch@ann.jussieu.fr

In the present paper, we show how to enforce the validity of the kinetic relation at the numerical level, and we design a *fully conservative* scheme which combines the advantages of standard finite differences and Glimm-type (see below) approaches.

Nonclassical shocks and other phase transitions are naturally present in many models of continuum physics, especially in the modeling of real fluids governed by complex equations of state. This is the case, for instance, of models describing the dynamics of liquid-vapor phase transitions in compressible fluids, or of solid-solid phase transformations in materials such as memory alloys. For numerical work in this direction we refer to [18, 19, 10, 31, 32].

Setting for this paper

We here restrict attention to scalar conservation laws

$$\begin{aligned} &\partial_t u + \partial_x f(u) = 0, \qquad u(x,t) \in \mathbb{R},\ (x,t) \in \mathbb{R} \times \mathbb{R}^+, \\ &u(x,0) = u_0(x), \end{aligned} \tag{1}$$

and postpone the discussion of systems of conservation laws. The above equation must be supplemented with an entropy inequality of the form

$$\partial_t U(u) + \partial_x F(u) \leqslant 0. \tag{2}$$

Here, t denotes the time variable, x the (one-dimensional) space variable, $f : \mathbb{R} \to \mathbb{R}$ the flux function, and (U, F) is any strictly convex mathematical entropy pair. That is, $U : \mathbb{R} \to \mathbb{R}$ is strictly convex and $F : \mathbb{R} \to \mathbb{R}$ is given by $F' = U' f'$. Equations (1) and (2) are imposed in the distributional sense.

We rely here on the theory of nonclassical solutions based on kinetic relations, established in [24]. The flux f is assumed to be *nonconvex,* which is the source of mathematical and numerical difficulties. From the mathematical standpoint, a single entropy inequality like (2) does not suffice to select a unique solution. This can be seen already at the level of the Riemann problem, corresponding to (1)-(2) when u_0 has the piecewise constant form

$$u_0(x) = \begin{cases} u_l, & x < 0, \\ u_r, & x > 0, \end{cases} \tag{3}$$

u_l and u_r being constant states. The Riemann problem admits (up to) a one-parameter family of solutions (see Chapter 2 in [24]). However, these solutions contain discontinuities violating the standard Lax shock inequalities, which are referred to as *nonclassical*. They are essential from the physical standpoint, and should be retained. This nonuniqueness can, however, be fixed provided an additional algebraic condition, the so-called *kinetic relation,* is imposed on each nonclassical shock. Consider a shock connecting a left-hand state u_- to a right-hand state u_+ and propagating with the speed σ given by the usual Rankine–Hugoniot relation, that is,

$$u(x,t) = \begin{cases} u_-, & x < \sigma t, \\ u_+, & x > \sigma t, \end{cases} \qquad \sigma = \sigma(u_-, u_+) = \frac{f(u_+) - f(u_-)}{u_+ - u_-}. \tag{4}$$

The kinetic relation takes the form

$$u_+ = \varphi^\flat(u_-) \quad \text{for all nonclassical shocks,} \tag{5}$$

where $\varphi^\flat$ is the so-called *kinetic function*. Equivalently, denoting by $\varphi^{-\flat}$ the inverse of the kinetic function it may be preferable to write $u_- = \varphi^{-\flat}(u_+)$. The kinetic relation implies that the right-hand (respectively left-hand) state is no longer free (as in a classical shock wave) but depends explicitly on the left-hand (respectively right-hand) state.

Objectives of this paper

At the numerical level, several strategies exist in the literature in order to take into account the kinetic relation (5). We can distinguish between diffuse interface methods and sharp interface methods.

In the first approach, one assumes that the kinetic relation is derived from an augmented continuous model and, in order to take into account the internal structure of nonclassical discontinuities, one attempts to resolve the effects due to (small) diffusive and dispersive terms that generate them. It is then possible to construct conservative schemes that mimic at the numerical level the effect of the regularized models. Due to the great sensitivity of nonclassical solutions with respect to small scales and numerical diffusion, it turns out that numerical results are satisfactory for shocks with moderate amplitude, but discrepancies between the exact and the numerical kinetic function arise for shocks with large amplitudes and in long-time computations. For this circle of ideas we refer the reader to [15, 16], and the follow-up papers [26, 9, 10].

In the second approach, small scale features are not explicitly taken into account. Instead, the kinetic relation is included, in a way or another, in the design of the numerical scheme. This is the case of the random choice and front tracking schemes. It should be mentioned here that the Glimm scheme and front tracking schemes do converge to exact solutions even in presence of nonclassical shocks; see [23, 24, 27] for the theoretical aspects and Chalons and LeFloch [11] for a numerical study of the Glimm scheme. These schemes require the explicit knowledge of the underlying nonclassical Riemann solver, which may be expensive numerically, and this motivated the introduction of the so-called transport-equilibrium scheme in Chalons [7, 8].

In [19], Hou, LeFloch, and Zhong proposed a class of converging schemes for the computation of propagating solid-solid phase boundaries and, more recently, Merckle and Rohde [32] developed a ghost-fluid type algorithm for a model of dynamics of phase transition. Those schemes provide satisfactory numerical results, as nonclassical discontinuities are sharply and accurately computed. The convergence of the methods was demonstrated numerically; however, their drawback is similar to the Glimm-type schemes since the strict conservation property in the conservative variable fails to hold.

Building on these previous works, our objective in this paper is to design a fully conservative, finite difference scheme for the approximation of nonclassical solutions to the hyperbolic conservation law (1). We rely on the discontinuous reconstruction technique proposed recently in Lagoutière [21, 22] which has been found to be particularly efficient for computing *classical* solutions of (1) with moderate numerical diffusion.

In our approach proposed below, the kinetic function $\varphi^\flat$ is included explicitly in the algorithm, in such a way that nonclassical shocks are computed *exactly,* while classical shocks suffer moderate numerical diffusion. To validate our strategy we perform various numerical experiments and, in particular, we draw the kinetic function associated with our scheme. As the mesh is refined, we observe that the approximate kinetic function converges toward the analytic kinetic function. The scheme also enjoys several fundamental stability properties of consistency with the conservative form of the equation and (like the Glimm scheme) with single nonclassical discontinuities.

2. Nonclassical Riemann solver with kinetics

Assumption on the flux function

We describe here the nonclassical Riemann solver introduced and investigated in LeFloch [24]. Note in passing that this solver was later extended in [27] to include also a nucleation criterion. One considers the problem (1)-(2)-(5) for a given Riemann initial data (3). Throughout this paper we assume that the flux f is either *concave-convex* or *convex-concave*, that is, satisfies the conditions (for all $u \neq 0$)

$$uf''(u) > 0, \qquad f'''(0) \neq 0, \qquad \lim_{|u|\to+\infty} f'(u) = +\infty, \tag{6}$$

or

$$uf''(u) < 0, \qquad f'''(0) \neq 0, \qquad \lim_{|u|\to+\infty} f'(u) = -\infty, \tag{7}$$

respectively. The functions $f(u) = u^3 + u$ and $f(u) = -u^3 - u$ are prototypes of particular interest, used later in this paper for the validation of the proposed numerical strategy.

Let $\varphi^\natural : \mathbb{R} \to \mathbb{R}$ be the unique function defined by $\varphi^\natural(0) = 0$ and for all $u \neq 0$, $\varphi^\natural(u) \neq u$ is such that the line passing through the points $(u, f(u))$ and $(\varphi^\natural(u), f(\varphi^\natural(u)))$ is tangent to the graph of f at the point $(\varphi^\natural(u), f(\varphi^\natural(u)))$:

$$f'(\varphi^\natural(u)) = \frac{f(u) - f(\varphi^\natural(u))}{u - \varphi^\natural(u)}.$$

This function is smooth, decreasing and onto thanks to (6) or (7). We denote by $\varphi^{-\natural} : \mathbb{R} \to \mathbb{R}$ its inverse function.

Concave-convex flux functions

Assume that f obeys (6) and let $\varphi^\flat : \mathbb{R} \to \mathbb{R}$ be a kinetic function, that is (by definition), a decreasing and Lipschitz continuous mapping such that

$$\begin{aligned} &\varphi_0^\flat(u) < \varphi^\flat(u) \leqslant \varphi^\natural(u), \quad u > 0, \\ &\varphi^\natural(u) \leqslant \varphi^\flat(u) < \varphi_0^\flat(u), \quad u < 0. \end{aligned} \tag{8}$$

Here, $\varphi_0^\flat$ provides lower/upper bounds associated with the entropy dissipation function for the chosen entropy function. (See [24] for details.) From $\varphi^\flat$ we define the function $\varphi^\sharp : \mathbb{R} \to \mathbb{R}$ such that the line passing through the points $(u, f(u))$ and $(\varphi^\flat(u), f(\varphi^\flat(u)))$ with $u \neq 0$ also cuts the graph of the flux function f at the point $(\varphi^\sharp(u), f(\varphi^\sharp(u)))$ with $\varphi^\sharp(u) \neq u$ and $\varphi^\sharp(u) \neq \varphi^\flat(u)$:

$$\frac{f(u) - f(\varphi^\flat(u))}{u - \varphi^\flat(u)} = \frac{f(u) - f(\varphi^\sharp(u))}{u - \varphi^\sharp(u)}.$$

The nonclassical Riemann solver associated with (1)-(2)-(3)-(5) is given as follows. When $u_l > 0$:

(1) If $u_r \geqslant u_l$, the solution is a rarefaction wave connecting u_l to u_r.
(2) If $u_r \in [\varphi^\sharp(u_l), u_l)$, the solution is a classical shock wave connecting u_l to u_r.
(3) If $u_r \in (\varphi^\flat(u_l), \varphi^\sharp(u_l))$, the solution contains a nonclassical shock connecting u_l to $\varphi^\flat(u_l)$, followed by a classical shock connecting $\varphi^\flat(u_l)$ to u_r.
(4) If $u_r \leqslant \varphi^\flat(u_l)$, the solution contains a nonclassical shock connecting u_l to $\varphi^\flat(u_l)$, followed by a rarefaction connecting $\varphi^\flat(u_l)$ to u_r.

When $u_l \leqslant 0$:

(1) If $u_r \leqslant u_l$, the solution is a rarefaction wave connecting u_l to u_r.
(2) If $u_r \in [u_l, \varphi^\sharp(u_l))$, the solution is a classical shock wave connecting u_l to u_r.
(3) If $u_r \in (\varphi^\sharp(u_l), \varphi^\flat(u_l))$, the solution contains a nonclassical shock connecting u_l to $\varphi^\flat(u_l)$, followed by a classical shock connecting $\varphi^\flat(u_l)$ to u_r.
(4) If $u_r \geqslant \varphi^\flat(u_l)$, the solution contains a nonclassical shock connecting u_l to $\varphi^\flat(u_l)$, followed by a rarefaction connecting $\varphi^\flat(u_l)$ to u_r.

Convex-concave flux functions

We next assume that f satisfies the condition (7). Let $\varphi^\flat : \mathbb{R} \to \mathbb{R}$ be a kinetic function, that is, a decreasing and Lipschitz continuous map such that

$$\begin{aligned} &\varphi_0^\flat(u) < \varphi^\flat(u) \leqslant \varphi^{-\natural}(u), \quad u < 0, \\ &\varphi^{-\natural}(u) \leqslant \varphi^\flat(u) < \varphi_0^\flat(u), \quad u > 0. \end{aligned} \tag{9}$$

We then define $\rho(u, v) \in \mathbb{R}$ if $v \neq u$ and $v \neq \varphi^\natural(u)$ by

$$\frac{f(\rho(u, v)) - f(u)}{\rho(u, v) - u} = \frac{f(v) - f(u)}{v - u}$$

whenever $\rho(u, v) \neq u$ and $\rho(u, v) \neq v$, and extend the function ρ by continuity elsewhere. Note that $\varphi^\sharp(u) = \rho(u, \varphi^\flat(u))$ where $\varphi^\sharp$ is defined as in the case of a concave-convex flux function. The nonclassical Riemann solver associated with (1)-(2)-(3)-(5) is given as follows. When $u_l > 0$:

(1) If $u_r \geqslant u_l$, the solution is a classical shock connecting u_l to u_r.
(2) If $u_r \in [0, u_l)$, the solution is a rarefaction wave connecting u_l to u_r.
(3) If $u_r \in (\varphi^\flat(u_l), 0)$, the solution contains a rarefaction wave connecting u_l to $\varphi^{-\flat}(u_r)$, followed by a nonclassical shock connecting $\varphi^{-\flat}(u_r)$ to u_r.
(4) If $u_r \leqslant \varphi^\flat(u_l)$, the solution contains:
   (i) a classical shock connecting u_l to $\varphi^{-\flat}(u_r)$, followed by a nonclassical shock connecting $\varphi^{-\flat}(u_r)$ to u_r, if $u_l > \rho(\varphi^{-\flat}(u_r), u_r)$;
   (ii) a classical shock connecting u_l to u_r, if $u_l \leqslant \rho(\varphi^{-\flat}(u_r), u_r)$.

When $u_l \leqslant 0$:

(1) If $u_r \leqslant u_l$, the solution is a classical shock connecting u_l to u_r.
(2) If $u_r \in (u_l, 0]$, the solution is a rarefaction wave connecting u_l to u_r.
(3) If $u_r \in (0, \varphi^\flat(u_l))$, the solution contains a rarefaction wave connecting u_l to $\varphi^{-\flat}(u_r)$, followed by a non classical shock connecting $\varphi^{-\flat}(u_r)$ to u_r.
(4) If $u_r \geqslant \varphi^\flat(u_l)$, the solution contains:
   (i) a classical shock connecting u_l to $\varphi^{-\flat}(u_r)$, followed by a nonclassical shock connecting $\varphi^{-\flat}(u_r)$ to u_r, if $u_l < \rho(\varphi^{-\flat}(u_r), u_r)$;
   (ii) a classical shock connecting u_l to u_r, if $u_l \geqslant \rho(\varphi^{-\flat}(u_r), u_r)$.

Observe that the convex-concave case can in principle be deduced from the concave-convex case, by replacing f by $-f$ and x by $-x$. Nevertheless, it is useful to keep the above two descriptions

in mind, since there is a dramatic difference between the Riemann solvers: the nonclassical shock always connects u_l to $\varphi^\flat(u_l)$ in the concave-convex case, and $\varphi^{-\flat}(u_r)$ to u_r in the convex-concave case. The numerical method we are going to describe must take this feature into account, and as we will explain it is necessary to take into account both $\varphi^\flat$ and $\varphi^{-\flat}$ in the design of the scheme.

3. Motivations and difficulties

Notation

Our aim is to design a scheme for the numerical approximation of the nonclassical solutions to (1)-(2)-(5). To this end, we consider the general class of finite volume methods. Introducing constant space and time lengths Δx and Δt for the space and time discretization, we can set $x_{j+1/2} = j\Delta x$, $j \in \mathbb{Z}$, and $t^n = n\Delta t$, $n \in \mathbb{N}$. The discretization consists, at each time t^n, of a piecewise constant function $x \mapsto u_\nu(x, t^n)$ which should be an approximation of the exact solution $u(x, t^n)$ on the cell $\mathcal{C}_j = [x_{j-1/2}, x_{j+1/2})$:

$$u_\nu(x, t^n) = u_j^n, \qquad x \in C_j,\ j \in \mathbb{Z},\ n \in \mathbb{N}.$$

Here, ν refers to the ratio $\Delta t/\Delta x$. The initial data at time $t = 0$ is denoted by u_0 and we define the sequence $(u_j^0)_{j\in\mathbb{Z}}$ by

$$u_j^0 = \frac{1}{\Delta x}\int_{x_{j-1/2}}^{x_{j+1/2}} u_0(x)\,\mathrm{d}x, \qquad j \in \mathbb{Z}. \tag{10}$$

The starting point in the idea of our algorithm is an unconventional interpretation of the constant values u_j^n, $j \in \mathbb{Z}$. As suggested by the proposed initialization (10), u_j^n is usually, and rightly, seen as an approximate value of the average on the cell $\mathcal{C}_j$ of the exact solution at time t^n. Integrating equation (1) over the slab $\mathcal{C}_j \times [t^n, t^{n+1}]$ and using Green's formula, it is thus natural to define $(u_j^{n+1})_j$ from $(u_j^n)_j$ and a conservative scheme of the form

$$u_j^{n+1} = u_j^n - \frac{\Delta t}{\Delta x}(f_{j+1/2}^n - f_{j-1/2}^n), \quad j \in \mathbb{Z}, \tag{11}$$

where $f_{j+1/2}^n$ represents an approximate value of the flux that passes through the interface $x_{j+1/2}$ between times t^n and t^{n+1}.

Here, we also consider u_j^n as a given piece of information, on the cell $\mathcal{C}_j$ and at time t^n, about the structure of the exact Riemann solution associated with the inital states $u_l = u_{j-1}^n$ and $u_r = u_{j+1}^n$, which develop later at time $t > t^n$. At this stage, one realizes that if this information is sufficiently sharp (i.e. close to what really happens), then we should be in a good position to define the numerical fluxes $f_{j+1/2}^n$ accurately and predict the approximate values of the solution at time t^{n+1}.

Linear advection equation

As a first illustration, let us consider the linear advection with constant velocity $a > 0$, that is, the scalar conservation law with flux $f(u) = au$. In this case, the weak solution to the initial-value problem for (1) is unique, and is given explicitly as $u(x, t) = u_0(x - at)$. Hence, neither the entropy condition (2) nor the kinetic condition (5) are necessary. The basic scheme for approximating this solution is the so-called upwind scheme and corresponds to the choice $f_{j+1/2}^n = au_j^n$ for all $j \in \mathbb{Z}$. Recall that the CFL condition $a\Delta t/\Delta x \leqslant \alpha$ for a given $\alpha \leqslant 1$ is mandatory for the stability of

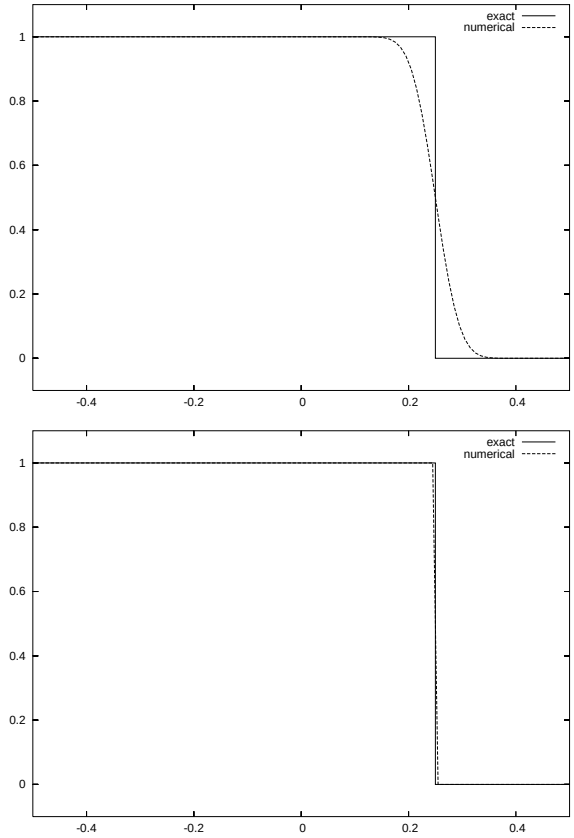

FIG. 1. Linear advection: upwind scheme (top) and reconstruction scheme (bottom).

the procedure. Figure 1 (top) shows the corresponding numerical is in solution at time $t = 0.25$ for $a = 1, \alpha = 0.5$ and $u_l = 1, u_r = 0$ in (3). The mesh contains 100 points per unit. We observe that the numerical solution is in good agreement with the exact one but contains numerical diffusion. We propose the following interpretation. In some sense, the value u_j^n that we consider as information on the Riemann solution associated with initial states $u_l = u_{j-1}^n$ and $u_r = u_{j+1}^n$ is sufficient to correctly approach this solution when defining $f_{j+1/2}^n = au_j^n$, but not enough to avoid the numerical diffusion. Note that the latter is expected but not desired. In the present situation, the fact is that we actually know what will happen in the future, namely propagation of the Riemann initial states ($u_l = u_{j-1}^n$ and $u_r = u_{j+1}^n$) with speed a. In particular, no value different from u_{j-1}^n and u_{j+1}^n is created so that the information given by u_j^n is clearly not optimal. In the process of calculation of the numerical flux $f_{j+1/2}^n$, we are thus tempted to add more information in the cell $\mathcal{C}_j$ by replacing, as soon as possible, the constant state u_j^n with a discontinuity separating u_{j-1}^n on the left and u_{j+1}^n on the right, and located at a point $\overline{x}_j \in \mathcal{C}_j$. In the forthcoming developments, the left and right states of this reconstructed discontinuity will be denoted by $u_{j,l}^n$ and $u_{j,r}^n$, respectively. Hence, we have here

$$u_{j,l}^n = u_{j-1}^n, \quad u_{j,r}^n = u_{j+1}^n. \tag{12}$$

See Figure 2 below. We claim that this provides better information for calculating $f^n_{j+1/2}$ than the original one. Such a reconstruction has to conserve u in order to be relevant, which defines $\overline{x}_j$ by the following constraint:

$$(\overline{x}_j - x_{j-1/2})u^n_{j,l} + (x_{j+1/2} - \overline{x}_j)u^n_{j,r} = (x_{j+1/2} - x_{j-1/2})u^n_j,$$

which equivalently recasts as

$$\overline{x}_j = x_{j-1/2} + \frac{u^n_{j,r} - u^n_j}{u^n_{j,r} - u^n_{j,l}}\Delta x. \tag{13}$$

Then the reconstruction is possible provided we have $0 \leqslant d^n_j \leqslant 1$ where

$$d^n_j = \frac{u^n_{j,r} - u^n_j}{u^n_{j,r} - u^n_{j,l}}. \tag{14}$$

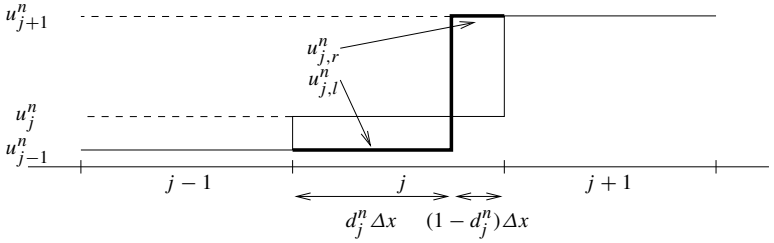

FIG. 2. An example of discontinuous reconstruction with conservation property (the linear case).

Now, let us introduce $\Delta t_{j+1/2}$, the time needed by the reconstructed discontinuity to reach the interface $x_{j+1/2}$ (recall that $a > 0$). We clearly have

$$\Delta t_{j+1/2} = \frac{1 - d^n_j}{a}\Delta x.$$

In this case, the flux that passes through $x_{j+1/2}$ between times t^n and $t^{n+1} = t^n + \Delta t$ equals $f(u^n_{j,r})$ until $t^n + \Delta t_{j+1/2}$, and $f(u^n_{j,l})$ after (if $\Delta t_{j+1/2} < \Delta t$). Therefore, we propose to set now

$$\Delta t f^n_{j+1/2} = \min(\Delta t_{j+1/2}, \Delta t) f(u^n_{j,r}) + \max(\Delta t - \Delta t_{j+1/2}, 0) f(u^n_{j,l}).$$

In Figure 1 (bottom), we have plotted the numerical solution given by this new numerical flux, leading to the so-called reconstruction scheme. The parameters of the simulation are the same as those of Figure 1 (top). We see that the more precise information we have brought on each cell $\mathcal{C}_j$ for calculating the numerical fluxes makes the scheme less diffusive than the original one. This strategy was proposed (and further discussed in detail) in [21, 22] (see also [12, 20]). In particular, it is shown therein that the numerical solution presented in Figure 1 (bottom) is *exact* in the sense that u^n_j equals the average of the exact solution on $\mathcal{C}_j$, that is,

$$u^n_j = \frac{1}{\Delta x}\int_{x_{j-1/2}}^{x_{j+1/2}} u(x, t^n)\,\mathrm{d}x, \qquad j \in \mathbb{Z},\ n \in \mathbb{N}. \tag{15}$$

The corresponding numerical discontinuity separating u_l and u_r is then diffused on one cell at most.

Godunov scheme with a nonclassical Riemann solver

As a second illustration, let us go back to the problem (1)-(2)-(5) with a general concave-convex (or convex-concave) flux function f with, however, for the sake of clarity,

$$f'(u) \geqslant 0, \qquad u \in \mathbb{R}. \tag{16}$$

Here, we focus on a particular Riemann initial data (3) such that $u_r = \varphi^\flat(u_l)$. In other words, the kinetic criterion is imposed on the initial discontinuity. The exact solution then corresponds to the propagation of this discontinuity with speed $\sigma(u_l, u_r) > 0$ given by the Rankine–Hugoniot relation:

$$\sigma(u_l, u_r) = \frac{f(u_r) - f(u_l)}{u_r - u_l}. \tag{17}$$

Figure 3 (top) represents the numerical solution given by the upwind scheme $f^n_{j+1/2} = f(u^n_j)$ at time $t = 0.1$, for $f(u) = u^3 + u$ and $u_l = 1$. The kinetic function is taken to be $\varphi^\flat(u) = -0.75\,u$ so that $u_r = -0.75$.

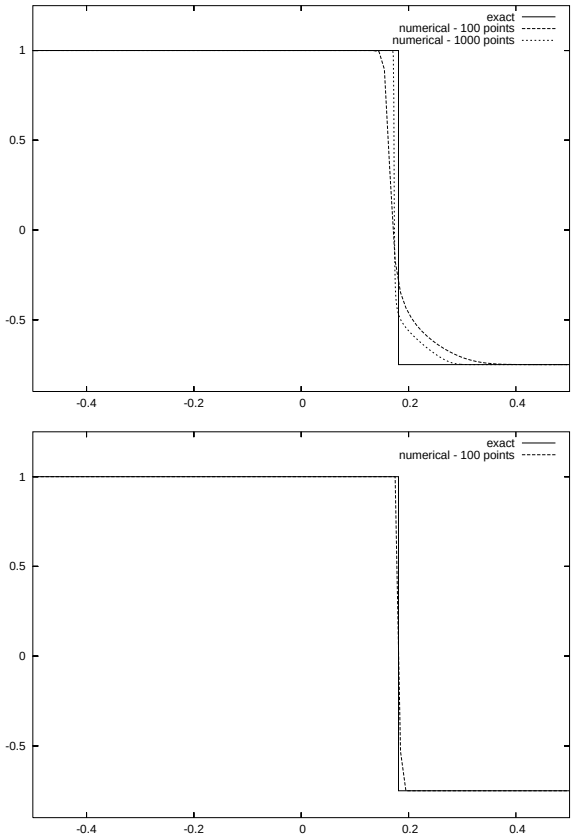

FIG. 3. Propagating nonclassical shock: upwind scheme (top) and reconstruction scheme (bottom).

We observe a strong disagreement between the numerical solution and the exact one. Indeed, the former is made of a (classical) shock followed by a rarefaction wave while the latter is a single (nonclassical) shock from u_l to u_r. It is then clear that the usual upwind scheme (as many others actually) is not adapted for the computation of nonclassical solutions. The next result states that the upwind scheme always converges towards the classical solution of (1)-(2). This scheme is then adapted for the computation of classical solutions only.

PROPERTY Assume that $u_0 \in L^\infty(\mathbb{R})$ and f is a smooth function satisfying (16). Then, under the CFL condition

$$\frac{\Delta t}{\Delta x} \max_{u \in A} |f'(u)| \leqslant 1$$

with $A := [\min_x u_0(x), \max_x u_0(x)]$, the upwind conservative scheme (11) with $f^n_{j+1/2} = f(u^n_j)$ converges towards the unique classical solution of (1)-(2).

To establish this property, we only need to observe that, under the assumption (16) (propagation is only in one direction), the upwind scheme is equivalent to the standard Godunov scheme associated with the *classical* Riemann solver of (1)-(2). Then standard compactness and consistency arguments apply and allow us to conclude that the scheme converges towards the unique classical solution. Obviously, the property also holds if f is decreasing, provided we define $f^n_{j+1/2} = f(u^n_{j+1})$.

4. A conservative scheme for nonclassical entropy solutions

Preliminaries

In view of the discussion in the previous section and in order to better evaluate the numerical fluxes $f^n_{j+1/2}$, let us obtain some information beyond u^n_j on the cell $\mathcal{C}_j$. In the case of an isolated propagating discontinuity, it is expected that the Riemann solution associated with the initial states u^n_{j-1} and u^n_{j+1} simply propagates the initial discontinuity. This holds true if $u^n_{j-1} = u_l$ and $u^n_{j+1} = \varphi^\flat(u_l)$, or more generally if $u^n_{j+1} = \varphi^\flat(u^n_{j-1})$. Here again, we propose to replace the constant state u^n_j with a discontinuity separating $u^n_{j,l}$ and $u^n_{j,r}$, located at the point $\overline{x}_j$ given by (13), whenever possible, i.e. when $0 \leqslant d^n_j \leqslant 1$. So, we take

$$u^n_{j,l} = \varphi^{-\flat}(u^n_{j+1}) \quad \text{and} \quad u^n_{j,r} = \varphi^\flat(u^n_{j-1}). \tag{18}$$

Note that this reconstruction is equivalent to (12) provided that $u^n_{j-1} = u_l$ and $u^n_{j+1} = \varphi^\flat(u_l)$, or more generally $u^n_{j+1} = \varphi^\flat(u^n_{j-1})$. Then, under the assumption (16), we again set

$$\Delta t f^n_{j+1/2} = \min(\Delta t_{j+1/2}, \Delta t) f(u^n_{j,r}) + \max(\Delta t - \Delta t_{j+1/2}, 0) f(u^n_{j,l})$$

with now

$$\Delta t_{j+1/2} = \frac{1 - d^n_j}{\sigma(u^n_{j,l}, u^n_{j,r})} \Delta x. \tag{19}$$

Figure 3 (bottom) highlights the benefit of such a reconstruction. The numerical solution now fully agrees with the exact one, and moreover is free of numerical diffusion (the profile is composed of a single point). We will show below that it is exact in this case, in the sense that (15) is still valid as in the linear case.

The proposed scheme

In view of the above motivations and illustrations, we proceed to descibe our algorithm in the general case. Assuming a sequence $(u_j^n)_{j\in\mathbb{Z}}$ given at time t^n, it is a question of defining its evolution until the next time level t^{n+1}. In the context of a finite volume conservative scheme, we have to define the numerical fluxes $(f_{j+1/2}^n)_{j\in\mathbb{Z}}$ coming in (11). To this end, we still assume

$$\text{either} \quad f'(u) \geqslant 0 \text{ for all } u, \quad \text{or} \quad f'(u) \leqslant 0 \text{ for all } u, \tag{20}$$

so that propagation is in one direction only. According to the previous section, information in the cell $\mathcal{C}_j$ is understood as an element of the inner structure of the Riemann problem associated with the initial states u_{j-1}^n and u_{j+1}^n. It will be used to compute either $f_{j+1/2}^n$ (if $f'(u) \geqslant 0$) or $f_{j-1/2}^n$ (if $f'(u) \leqslant 0$).

In Section 2, it is shown that the Riemann problem associated with the initial states u_{j-1}^n and u_{j+1}^n may contain a nonclassical shock between u_{j-1}^n and $\varphi^\flat(u_{j-1}^n)$ if it is concave-convex (and between $\varphi^{-\flat}(u_{j+1}^n)$ and u_{j+1}^n if the function is convex-concave).

Recall that these nonclassical waves are difficult to capture numerically and require special attention. (We have shown in the previous section that as many others, the upwind scheme is unsuitable.) Instead of considering u_j^n as a sufficiently accurate information on the structure of the Riemann solution associated with the initial states u_{j-1}^n and u_{j+1}^n, we propose to replace it (whenever possible) with a discontinuity separating $u_{j,l}^n = \varphi^{-\flat}(u_{j+1}^n)$ on the left and $u_{j,r}^n = \varphi^\flat(u_{j-1}^n)$ on the right, and located at a point $\overline{x}_j \in \mathcal{C}_j$. In other words, we propose to introduce in the cell $\mathcal{C}_j$ the right (respectively left) state $\varphi^\flat(u_{j-1}^n)$ (respectively $\varphi^{-\flat}(u_{j+1}^n)$) of the nonclassical discontinuity which is expected to be present in the Riemann solution associated with u_{j-1}^n and u_{j+1}^n (depending on whether f obeys (6) or (7)). As in the previous section, one requires the reconstructed discontinuity to satisfy the conservation property (13) and to be located inside $\mathcal{C}_j$, that is, $0 \leqslant d_j^n \leqslant 1$ with d_j^n given in (14). See Figure 4 for an illustration. Here, we let $u_{j,l}^n = u_{j,r}^n = u_j^n$ if d_j^n given in (14) does not belong to $[0, 1]$.

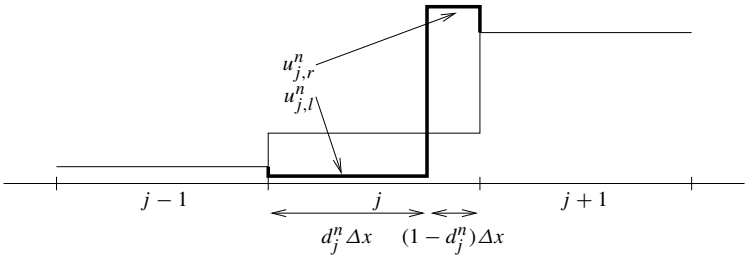

FIG. 4. A general discontinuous reconstruction with conservation property (the general case).

Then, we naturally set for all $j \in \mathbb{Z}$:

(i) if f is nondecreasing,

$$\Delta t f_{j+1/2}^n = \begin{cases} \min(\Delta t_{j+1/2}, \Delta t) f(u_{j,r}^n) + \max(\Delta t - \Delta t_{j+1/2}, 0) f(u_{j,l}^n), & 0 \leqslant d_j^n \leqslant 1, \\ \Delta t f(u_j^n), & \text{otherwise}, \end{cases} \tag{21}$$

with

$$\Delta t_{j+1/2} = \frac{1 - d_j^n}{\sigma(u_{j,l}^n, u_{j,r}^n)} \Delta x. \tag{22}$$

(ii) if f is nonincreasing,

$$\Delta t f_{j-1/2}^n = \begin{cases} \min(\Delta t_{j-1/2}, \Delta t) f(u_{j,l}^n) + \max(\Delta t - \Delta t_{j-1/2}, 0) f(u_{j,r}^n), & 0 \leqslant d_j^n \leqslant 1, \\ \Delta t f(u_j^n), & \text{otherwise}, \end{cases} \tag{23}$$

with

$$\Delta t_{j-1/2} = \frac{d_j^n}{-\sigma(u_{j,l}^n, u_{j,r}^n)} \Delta x. \tag{24}$$

Note that in contrast to the case of linear advection (see the first illustration in the previous section), the local time step $\Delta t_{j+1/2}$ (respectively $\Delta t_{j-1/2}$) given by (22) (respectively (24)) is now only a prediction of the time needed by the reconstructed discontinuity to reach the interface $x_{j+1/2}$ (respectively $x_{j-1/2}$). The prediction step is, however, exact in the case of an isolated nonclassical discontinuity (see the second illustration in the previous section) and more generally as soon as u_{j-1}^n and u_{j+1}^n satisfy $u_{j+1}^n = \varphi^\flat(u_{j-1}^n)$.

Observe that the proposed scheme belongs to the class of five-point schemes, since u_j^{n+1} depends on u_{j-2}^n, u_{j-1}^n, u_j^n, u_{j+1}^n and u_{j+2}^n.

Stability and consistency properties

We now state and prove important properties enjoyed by our algorithm.

We assume that the flux f satisfies the monotonicity condition (20) and either the concave-convex or concave-convex conditions (6) or (7) respectively. Then, under the CFL restriction

$$\frac{\Delta t}{\Delta x} \max_u |f'(u)| \leqslant 1, \tag{25}$$

where the maximum is taken over all the u under consideration, the conservative scheme (11) with $f_{j+1/2}^n$ defined for all $j \in \mathbb{Z}$ by (21)-(23) is consistent with (1)-(2)-(5) in the following sense.

PROPERTY 1 (Flux consistency) Assume that $u := u_{j-1}^n = u_j^n = u_{j+1}^n$. Then $f_{j+1/2}^n = f(u)$ if $f' \geqslant 0$ and $f_{j-1/2}^n = f(u)$ if $f' \leqslant 0$.

PROPERTY 2 (Classical solutions) Assume that u_{j-2}^n, u_{j-1}^n, u_j^n, u_{j+1}^n and u_{j+2}^n belong to the same region of convexity of f. Then the definition u_j^{n+1} given by the conservative scheme (11)-(21)-(23) coincides with the one given by the usual upwind conservative scheme, so it has all the usual stability properties provided by the latter scheme. In particular, the strategy is convergent if the whole discrete solution belongs to the same region of convexity of f.

PROPERTY 3 (Isolated nonclassical shock waves) Let u_l and u_r be two initial states such that $u_r = \varphi^\flat(u_l)$. Assume that $u_j^0 = u_l$ if $j \leqslant 0$ and $u_j^0 = u_r$ if $j \geqslant 1$. Then the conservative scheme (11)-(21)-(23) provides an exact numerical solution on each cell $\mathcal{C}_j$ in the sense that

$$u_j^n = \frac{1}{\Delta x} \int_{x_{j-1/2}}^{x_{j+1/2}} u(x, t^n)\, \mathrm{d}x, \qquad j \in \mathbb{Z},\ n \in \mathbb{N}, \tag{26}$$

where u denotes the exact Riemann solution of (1)-(2)-(3)-(5) given by $u(x,t) = u_l$ if $x < \sigma(u_l, u_r)t$ and $u(x,t) = u_r$ otherwise, and is convergent towards u. In particular, the numerical discontinuity is diffused on one cell at most.

The following comments are in order. Property 1 shows that the proposed numerical flux function is consistent in the classical sense of finite volume methods. Properties 2 and 3 provide us with crucial stability/accuracy properties. They show that the method is actually convergent if the solution remains in the same region of convexity of f (see Property 2) or, more importantly, the solution is an isolated nonclassical discontinuity satisfying the prescribed kinetic relation (see Property 3). We emphasize that all of the *conservative* schemes proposed so far in the literature violate the latter property.

Proof of Property 1. If $u := u_{j-1}^n = u_j^n = u_{j+1}^n$ then

$$d_j^n = \frac{\varphi^\flat(u) - u}{\varphi^\flat(u) - \varphi^{-\flat}(u)}.$$

The property $0 \leqslant d_j^n \leqslant 1$ means $\min(\varphi^{-\flat}(u), \varphi^\flat(u)) \leqslant u \leqslant \max(\varphi^{-\flat}(u), \varphi^\flat(u))$ and cannot hold, since u and $\varphi^\flat(u)$ do not have the same sign for all u. Thus, we obtain $f_{j+1/2}^n = f(u)$ if $f' \geqslant 0$ and $f_{j-1/2}^n = f(u)$ if $f' \leqslant 0$ by (21)-(23).

Proof of Property 2. Assume without restriction that $f' \geqslant 0$ and recall that $0 \leqslant d_{j-1}^n \leqslant 1$ and $0 \leqslant d_j^n \leqslant 1$ respectively means that $\min(\varphi^{-\flat}(u_j^n), \varphi^\flat(u_{j-2}^n)) \leqslant u_{j-1}^n \leqslant \max(\varphi^{-\flat}(u_j^n), \varphi^\flat(u_{j-2}^n))$ and $\min(\varphi^{-\flat}(u_{j+1}^n), \varphi^\flat(u_{j-1}^n)) \leqslant u_j^n \leqslant \max(\varphi^{-\flat}(u_{j+1}^n), \varphi^\flat(u_{j-1}^n))$. These inequalities are not valid since by definition u and $\varphi^\flat(u)$ do not belong to the same region of convexity of f. By (21)-(23), the numerical fluxes $f_{j\pm1/2}^n$ coincide with the usual upwind fluxes and the conclusion follows.

Proof of Property 3. First, note that there is no relevant reconstruction in the first iteration. Indeed, the property $0 \leqslant d_j^n \leqslant 1$ reads as follows if $j < 0$ or $j > 1$:

$$0 \leqslant d_j^n \leqslant 1 \quad \text{if and only if} \quad \begin{cases} \min(\varphi^{-\flat}(u_l), \varphi^\flat(u_l)) \leqslant u_l \leqslant \max(\varphi^{-\flat}(u_l), \varphi^\flat(u_l)), & j < 0, \\ \min(\varphi^{-\flat}(u_r), \varphi^\flat(u_r)) \leqslant u_r \leqslant \max(\varphi^{-\flat}(u_r), \varphi^\flat(u_r)), & j > 1, \end{cases}$$

which again cannot hold (see below), while if $j = 0$ or $j = 1$, the relation $u_r = \varphi^\flat(u_l)$ and definition (14) give

$$\begin{cases} d_j^n = \dfrac{u_r - u_l}{u_r - u_l} = 1, & j = 0, \\ d_j^n = \dfrac{u_r - u_r}{u_r - u_l} = 0, & j = 1, \end{cases}$$

so that the reconstruction takes place but is always trivial: $u_l = \varphi^{-\flat}(u_r)$ (respectively $u_r = \varphi^\flat(u_l)$) takes the whole cell associated with $j = 0$ (respectively $j = 1$).

Now, without loss of generality assume that f is nondecreasing and Δt is sufficiently small so that (25) holds. After one time step Δt, the exact solution is given by $u(x, \Delta t) = u_l$ if $x <$

$\sigma(u_l, u_r)\Delta t$ and $u(x, \Delta t) = u_r$ otherwise, and therefore

$$\frac{1}{\Delta x}\int_{x_{j-1/2}}^{x_{j+1/2}} u(x, \Delta t)\,\mathrm{d}x = \begin{cases} u_l, & j \leqslant 0, \\ u_r - \sigma(u_l, u_r)\dfrac{\Delta t}{\Delta x}(u_r - u_l), & j = 1, \\ u_r, & j > 1. \end{cases} \tag{27}$$

Taking into account the value of $\sigma(u_l, u_r)$ given by (17) we obtain

$$\frac{1}{\Delta x}\int_{x_{j-1/2}}^{x_{j+1/2}} u(x, \Delta t)\,\mathrm{d}x = \begin{cases} u_l - \dfrac{\Delta t}{\Delta x}(f(u_l) - f(u_l)), & j \leqslant 0, \\ u_r - \dfrac{\Delta t}{\Delta x}(f(u_r) - f(u_l)), & j = 1, \\ u_r - \dfrac{\Delta t}{\Delta x}(f(u_r) - f(u_r)), & j > 1, \end{cases} \tag{28}$$

that is,

$$u_j^1 = \frac{1}{\Delta x}\int_{x_{j-1/2}}^{x_{j+1/2}} u(x, \Delta t)\,\mathrm{d}x, \qquad j \in \mathbb{Z}. \tag{29}$$

This establishes the identity (26) for the first iterate at least.

Consider now the next time iteration. In view of the above discussion it is clear that only the cell $\mathcal{C}_1$ is going to be involved in the reconstruction step. Now, the main argument is that, by construction, the reconstructed discontinuity in this cell connects the expected states $\varphi^{-\flat}(u_2^1) = \varphi^{-\flat}(u_r) = u_l$ and $\varphi^{\flat}(u_0^1) = \varphi^{\flat}(u_l) = u_r$ and moreover, according to the conservation property (29), is located exactly at the point $x = \sigma(u_l, u_r)\Delta t$. Again, our reconstruction produces the exact solution at time $t = \Delta t$, which gives (26). To handle the second iterate we note that, thanks to Green's formula, the conservative scheme (11) with $f_{j+1/2}^n$ defined (for all $j \in \mathbb{Z}$) by (21)-(23) is equivalent to averaging the exact solution. The arguments are the same for other iterates, and therefore the derivation of (26) is completed.

5. Numerical experiments

We mostly consider here the flux $f(u) := u^3 + u$, thus f is concave-convex in the sense of the second section. For the entropy-entropy flux pair (U, F) required in (2), we use

$$U(u) := u^2, \qquad F(u) := \frac{3}{2}u^4 + u^2.$$

This function determines the zero-dissipation kinetic function. Easy calculations lead to explicit formulas for $\varphi^{\natural}$ and $\varphi^{-\natural}$:

$$\varphi^{\natural} = -\frac{u}{2}, \qquad \varphi^{-\natural} = -2u, \qquad \varphi_0^{\flat}(u) = -u.$$

Moreover, here we have $\varphi^{\sharp}(u) = -u - \varphi^{\flat}(u)$. The choice of the kinetic function $\varphi^{\flat}$ must be in agreement with relations (8) with $\varphi^{\natural}$ and $\varphi_0^{\flat}$ just calculated. Here, we will choose

$$\varphi^{\flat}(u) = -\beta u, \qquad \beta \in [0.5, 1)\,,$$

which, as observed in Bedjaoui and LeFloch [5], can be realized by an augmented model based on nonlinear diffusion and dispersion terms. In the following, we will take $\beta = 0.75$.

TEST A Let us demonstrate Property 3, which is concerned with the exact capture of isolated nonclassical shocks. Thus, consider the following nonclassical shock as a Riemann initial condition:

$$u_0(x) = \begin{cases} 4, & x < 0, \\ \varphi^\flat(4) = -3, & x > 0, \end{cases}$$

The numerical solution shown in Figure 5 is exact everywhere but in the single cell containing the nonclassical shock. (We sometimes use a piecewise constant representation in the figure, to make the interpretation of the numerical solutions easier.) However, as expected, the value in this cell coincides with the average of the corresponding exact solution (see (26)), and allows us (after reconstruction) to recover the *exact* location of the discontinuity (using the conservation property of the scheme). This property explains why the numerical solution stays sharp as time goes on.

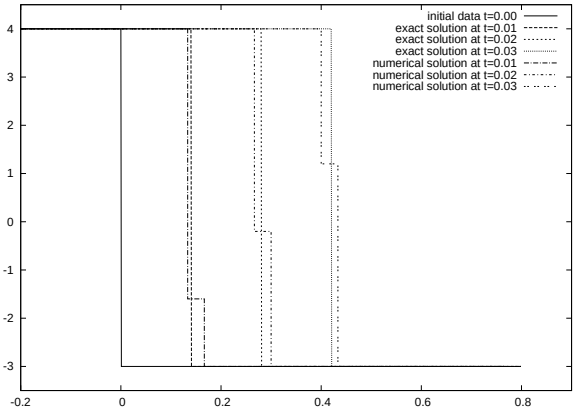

FIG. 5. Test A: Nonclassical shock, 30 points.

TEST B In our second test we consider the Riemann problem with initial data

$$u_0(x) = \begin{cases} 4, & x < 0, \\ -5, & x > 0, \end{cases}$$

whose solution is a nonclassical shock followed by a rarefaction wave. The two curves in Figure 6 (top) are performed with $\Delta x = 0.01$ and $\Delta x = 0.002$, respectively. The nonclassical shock, as previously, is localized in a single computational cell.

Figure 6 (bottom) represents the logarithm of the L^1-error (between the exact and the numerical solution) versus the logarithm of Δx. The numerical order of convergence is about 0.8374.

TEST C (Figure 7) Now, we choose another Riemann initial condition which develops a nonclassical shock followed by a classical shock:

$$u_0(x) = \begin{cases} 4, & x < 0, \\ -2, & x > 0. \end{cases}$$

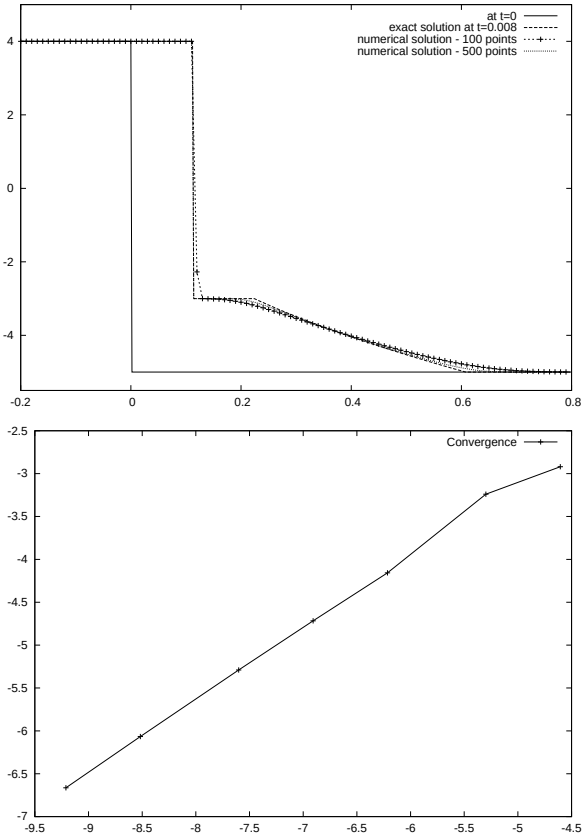

FIG. 6. Test B: Nonclassical shock and rarefaction, and L^1 convergence ($\log(E_{L^1})$ versus $\log(\Delta x)$).

We can make the same observation as previously, concerning the nonclassical shock; it is sharply captured and arises in a small spatial domain. However, here the classical shock does contain some numerical diffusion: in fact, our scheme is exactly the upwinding scheme if the values of the solution remain in a given convexity region for the flux f.

Once again, the plot with the L^1-error shows the numerical convergence with order about 0.9999.

TEST D (Figure 8) We now take an initial data composed of two nonclassical shocks that interact:

$$u_0(x) = \begin{cases} 4 = \varphi^{-\flat}(-3), & x < 0.1, \\ -3, & 0.1 < x < 0.2, \\ 2.25 = \varphi^{\flat}(-3), & x > 0.2. \end{cases}$$

The computation is performed with $\Delta x = 0.05$ and plotted at four successive times $t = 0, 0.0010, 0.0017$, and 0.0020. We observe that the two nonclassical shocks cancel each other at the interaction, and generate a single classical shock, in accordance with the general theory in [24].

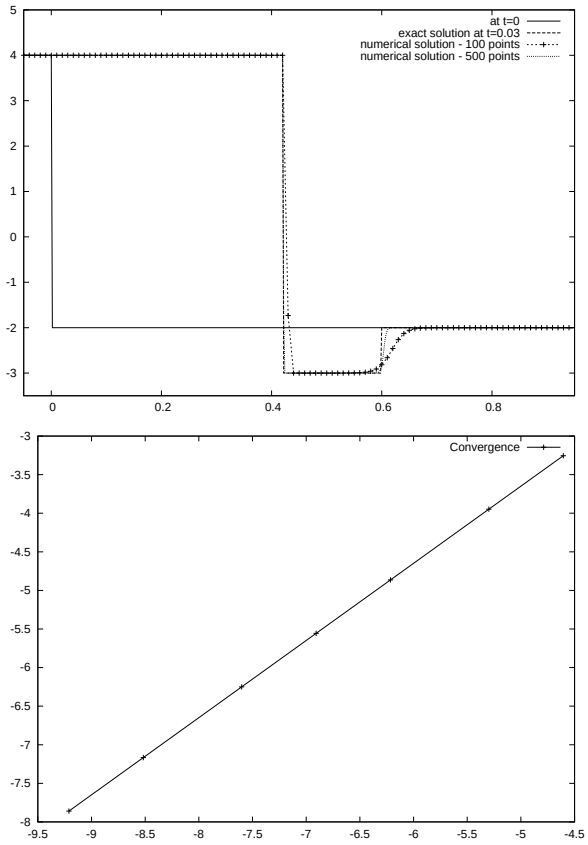

FIG. 7. Test C: Nonclassical and classical shocks, and L^1 convergence ($\log(E_{L^1})$ versus $\log(\Delta x)$).

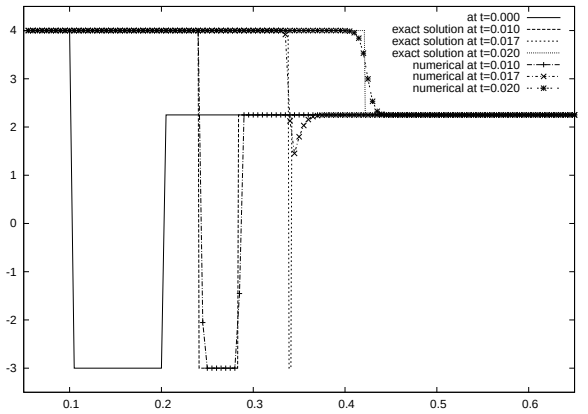

FIG. 8. Test D: Interaction of two nonclassical shocks.

TEST E (Figure 9) Next, we consider the periodic initial condition

$$u_0(x) = \sin\left(\frac{x}{2\pi}\right),$$

with periodic boundary conditions $u(-0.5, t) = u(0.5, t)$. The exact solution is not known explicitly, so we compare our numerical solution with the solution generated by Glimm's random choice scheme [14] in which we have replaced the classical solver by the nonclassical solver described in Section 2. We use here van der Corput's random sequence (a_n), defined by

$$a_n = \sum_{k=0}^{m} i_k 2^{-(k+1)},$$

where $n = \sum_{k=0}^{m} i_k 2^k$, $i_k \in \{0, 1\}$, denotes the binary expansion of the integer n. Figure 9 represents the solutions at times $t = 0, 0.25$ and 0.5 for our scheme with $\Delta x = 0.01$ and with $\Delta x = 0.0001$, and for the Glimm scheme with $\Delta x = 0.0001$ (to serve as a reference). The two methods strongly agree. Roughly speaking, the increasing parts of u_0 evolve as rarefactions, while

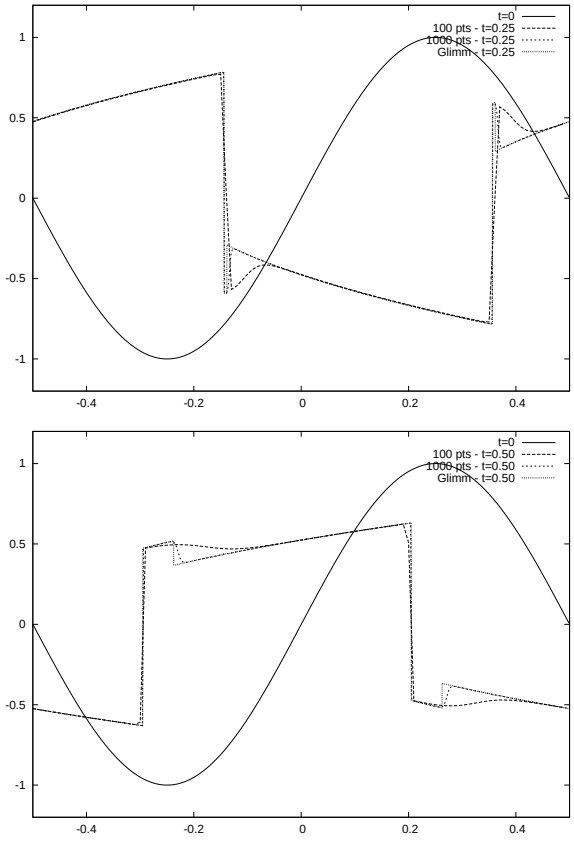

FIG. 9. Test E: Periodic initial data; reconstruction scheme and Glimm scheme.

the decreasing parts are compressed and develop a classical shock and, then, when left- and right-hand states at the shocks change sign, nonclassical shocks (which do satisfy the expected kinetic relation) and new faster classical shocks on the right-hand side arise.

TEST F (Figure 10) To illustrate the behavior of convex-concave flux functions, we finally compute two Riemann solutions with opposite flux $f(u) = -u^3 - u$ (so $f' < 0$ and the solutions move from right to left) and the same kinetic function $\varphi^\flat(u) = -0.75\ u$: the first one (top) corresponds to the initial data

$$u_0(x) = \begin{cases} -4, & x < 0, \\ 4, & x > 0, \end{cases}$$

and develops a rarefaction wave and a nonclassical shock; the second one (bottom) corresponds to the initial data

$$u_0(x) = \begin{cases} -2, & x < 0, \\ 4, & x > 0, \end{cases}$$

and the corresponding solution is a classical shock followed by a nonclassical shock.

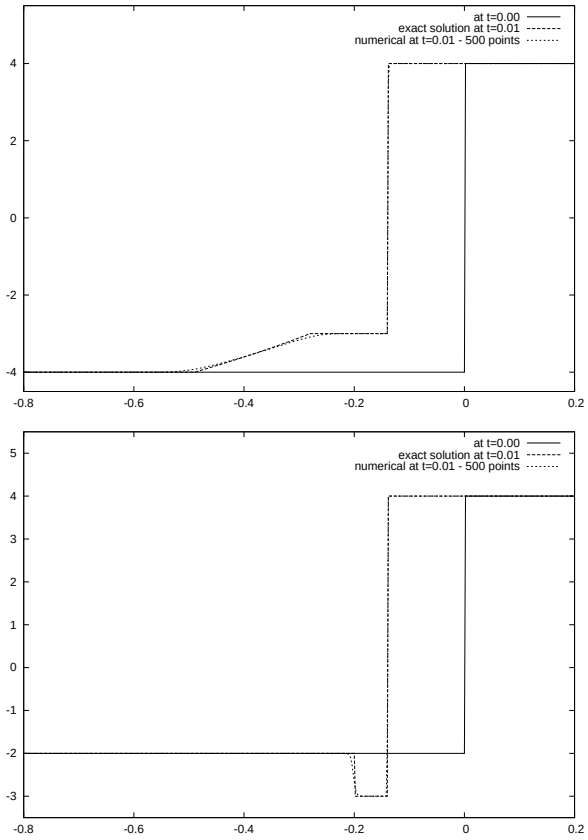

FIG. 10. Test F: Two examples in the convex-concave case.

TEST G We now study how the kinetic relation $u_R = \varphi^\flat(u_L)$ is computed. In Figure 11 (bottom), we plot points whose horizontal coordinates (respectively vertical coordinates) correspond to the left-hand (resp. right-hand) traces around the reconstructed cell. The initial data allows us to cover a large range of values:

$$u_0(x) = \begin{cases} 0, & x < -0.5, \\ 1 + 20(x + 0.45), & -0.5 < x < -0.45, \\ -0.75, & x > -0.45. \end{cases}$$

The top figure represents the solution at different times with $\Delta x = 0.0002$. No explicit form for the solution is available here. We clearly observe the convergence of the numerical kinetic relation towards the prescribed one (chosen here to be a linear function). We recall that the kinetic function characterizes the dynamics of nonclassical shocks; hence, this test definitely validates the proposed method.

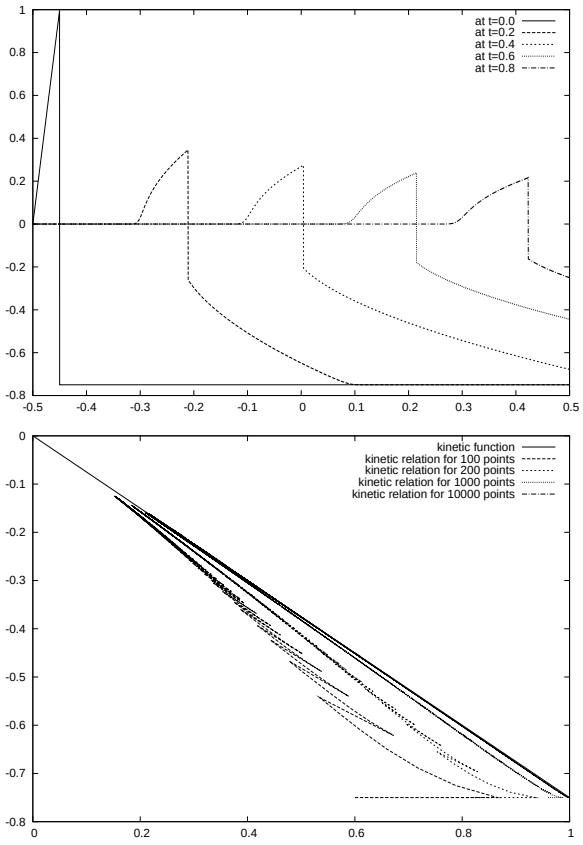

FIG. 11. Test G: Numerical kinetic relation.

TEST H In the course of designing the scheme proposed in the previous section we tried several variants. We report here one such scheme that is very similar to the proposed scheme, but which

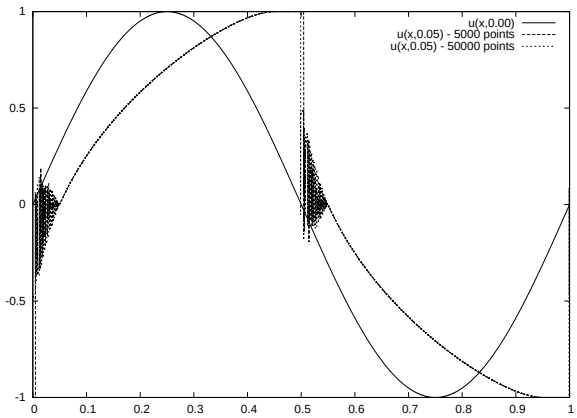

FIG. 12. Test H: Another version of the scheme.

does not converge to exact nonclassical solutions. This is due to the fact that small oscillations are generated in the scheme which are in competition with the dissipation mechanisms described by the prescribed kinetic function. The variant is designed for the concave-convex flux $f(u) = u^3 + u$. The only difference from the scheme developed above is that it performs the reconstruction in $\mathcal{C}_j$ with $u^n_{j,l} = u^n_{j-1}$ (instead of $\varphi^{-\flat}(u^n_{j+1})$ and $u_{j,r} = \varphi^{\flat}(u^n_{j-1})$. This is equivalent in the case of a *pure* nonclassical shock (Test B) but different in the general case.

Figure 12 presents the solution obtained for the same initial value as in Test E. Oscillations are generated because the reconstruction is not constrained enough in this version of the scheme.

6. Concluding remarks

In this paper we have introduced a new numerical strategy for computing nonclassical solutions to nonlinear hyperbolic conservation laws. The method is based on a reconstruction technique performed in each computational cell which may exhibit a nonclassical shock. Importantly, the whole algorithm is *conservative* and propagates any admissible nonclassical discontinuity exactly. The convergence of the proposed method was demonstrated numerically for several test cases. This new approach brings a new perspective to the numerical approximation of nonclassical shocks and kinetic functions. The efficiency of the method is clearly demonstrated in the present paper, and we refer to the follow-up paper [6] for various extensions. Among several open questions of interest we can mention the derivation of total variation bounds for the proposed scheme and generalization of our technique to hyperbolic systems of conservation laws, application to real materials undergoing phase transitions, as well as extension to higher-order schemes.

REFERENCES

1. ABEYARATNE, R., & KNOWLES, J. K. Kinetic relations and the propagation of phase boundaries in solids. *Arch. Ration. Mech. Anal.* **114** (1991), 119–154. Zbl 0745.73001 MR 1094433

2. ABEYARATNE, R., & KNOWLES, J. K. Implications of viscosity and strain gradient effects for the kinetics of propagating phase boundaries. *SIAM J. Appl. Math.* **51** (1991), 1205–1221. Zbl 0764.73013 MR 1127848

3. BEDJAOUI, N., & LEFLOCH, P. G. Diffusive-dispersive traveling waves and kinetic relations. III. A hyperbolic model of elastodynamics. *Ann. Univ. Ferrara Sci. Mat.* **47** (2001), 117–144. Zbl 1119.35340 MR 1897563

4. BEDJAOUI, N., & LEFLOCH, P. G. Diffusive-dispersive travelling waves and kinetic relations. II. A hyperbolic-elliptic model of phase-transition dynamics. *Proc. Roy. Soc. Edinburgh Sect. A* **132** (2002), 545–565. Zbl 1082.35104 MR 1912415

5. BEDJAOUI, N., & LEFLOCH, P. G. Diffusive-dispersive travelling waves and kinetic relations. V. Singular diffusion and nonlinear dispersion. *Proc. Roy. Soc. Edinburgh Sect. A* **134** (2004), 815–843. Zbl 1065.35182 MR 2099566

6. BOUTIN, B., CHALONS, C., LAGOUTIÈRE, F., & LEFLOCH, P. G. Convergent and conservative schemes for nonclassical solutions based on kinetic relations. II. Preprint (2008).

7. CHALONS, C. Transport-equilibrium schemes for computing nonclassical shocks. Scalar conservation laws. *Numer. Methods Partial Differential Equations* **24** (2008), 1127–1147. Zbl pre05303288

8. CHALONS, C. Numerical approximation of a macroscopic model of pedestrian flows. *SIAM J. Sci. Comput.* **29** (2007), 539–555. Zbl pre05256878 MR 2306257

9. CHALONS, C., & LEFLOCH, P. G. A fully discrete scheme for diffusive-dispersive conservation laws. *Numer. Math.* **89** (2001), 493–509. Zbl 1013.65096 MR 1864428

10. CHALONS, C., & LEFLOCH, P. G. High-order entropy conservative schemes and kinetic relations for van der Waals fluids. *J. Comput. Phys.* **168** (2001), 184–206. Zbl 1074.76583 MR 1826913

11. CHALONS, C., & LEFLOCH, P. G. Computing undercompressive waves with the random choice scheme. Nonclassical shock waves. *Interfaces Free Bound.* **5** (2003), 129–158. Zbl 1038.35134 MR 1979428

12. DESPRÉS, B., & LAGOUTIÈRE, F. Contact discontinuity capturing schemes for linear advection and compressible gas dynamics. *SIAM J. Sci. Comput.* **16** (2001), 479–524. Zbl 0999.76091 MR 1881855

13. FAN, H.-T., & SLEMROD, M. The Riemann problem for systems of conservation laws of mixed type. *Shock Induced Transitions and Phase Structures in General Media* (Minneapolis, MN, 1990), J. E. Dunn et al. (eds.), IMA Vol. Math. Appl. 52, Springer (1993), 61–91. Zbl 0807.76031 MR 1240333

14. GLIMM, J. Solutions in the large time for nonlinear hyperbolic systems of equations. *Comm. Pure Appl. Math.* **18** (1965), 697–715. Zbl 0141.28902 MR 0194770

15. HAYES, B. T., & LEFLOCH, P. G. Nonclassical shocks and kinetic relations: Scalar conservation laws. *Arch. Ration. Mech. Anal.* **139** (1997), 1–56. Zbl 0902.76053 MR 1475777

16. HAYES, B. T., & LEFLOCH, P. G. Nonclassical shocks and kinetic relations: Finite difference schemes. *SIAM J. Numer. Anal.* **35** (1998), 2169–2194. Zbl 0938.35096 MR 1655842

17. HAYES, B. T., & LEFLOCH, P. G. Nonclassical shock waves and kinetic relations: Strictly hyperbolic systems. *SIAM J. Math. Anal.* **31** (2000), 941–991. Zbl 0953.35095 MR 1759195

18. HOU, T. Y., LEFLOCH, P. G., & ROSAKIS, P. A level-set approach to the computation of twinning and phase transition dynamics. *J. Comput. Phys.* **150** (1999), 302–331. Zbl 0936.74052 MR 1684914

19. HOU, T. Y., LEFLOCH, P. G., & ZHONG, X. Converging methods for the computation of propagating solid-solid phase boundaries. *J. Comput. Phys.* **124** (1996), 192–216.

20. LAGOUTIÈRE, F., Modélisation mathématique et résolution numérique de problèmes de fluides compressibles à plusieurs constituants. Ph.D. thesis, Univ. Paris VI (2000).

21. LAGOUTIÈRE, F., Stability of reconstruction schemes for scalar hyperbolic conservation laws. *Comm. Math. Sci.* **6** (2008), 57–70. MR 2397997

22. LAGOUTIÈRE, F. Non-dissipative entropic discontinuous reconstruction schemes for hyperbolic conservation laws. Submitted.

23. LEFLOCH, P. G. Propagating phase boundaries: formulation of the problem and existence via the Glimm scheme. *Arch. Ration. Mech. Anal.* **123** (1993), 153–197. MR 1219421
24. LEFLOCH, P. G. *Hyperbolic Systems of Conservation Laws: The Theory of Classical and Nonclassical Shock Waves*, E.T.H. Lecture Notes Ser., Birkhäuser (2002). Zbl 1019.35001 MR 1927887
25. LEFLOCH, P. G., & MOHAMMADIAN, M. Why many shock wave theories are necessary. Fourth-order models, kinetic functions, and equivalent equations. *J. Comput. Phys.* **227** (2008), 4162–4189. Zbl pre05273734 MR 2403880
26. LEFLOCH, P. G., & ROHDE, C. High-order schemes, entropy inequalities, and nonclassical shocks. *SIAM J. Numer. Anal.* **37** (2000), 2023–2060. Zbl 0959.35117 MR 1766858
27. LEFLOCH, P. G., & SHEARER, M. Nonclassical Riemann solvers with nucleation. *Proc. Roy. Soc. Edinburgh Sect. A* **134** (2004), 941–964. Zbl 1090.35121
28. LEFLOCH, P. G., & THANH, M. D. Nonclassical Riemann solvers and kinetic relations I: A nonconvex hyperbolic model of phase transitions. *Z. Angew. Math. Phys.* **52** (2001), 597–619. Zbl 1020.35056 MR 1856989
29. LEFLOCH, P. G., & THANH, M. D. Nonclassical Riemann solvers and kinetic relations. II. An hyperbolic-elliptic model of phase transition dynamics. *Proc. Roy. Soc. Edinburgh Sect. A* **132** (2002), 181–219. Zbl 1021.35073 MR 1884477
30. LEFLOCH, P. G., & THANH, M. D. Properties of Rankine–Hugoniot curves for van der Waals fluids. *Japan J. Indust. Appl. Math.* **20** (2003), 211–238. Zbl 1044.76029 MR 1985510
31. MERKLE, C., & ROHDE, C. Computations of dynamical phase transitions in solids. *Appl. Numer. Math.* **56** (2006), 1450–1463. Zbl 1116.74049 MR 2245467
32. MERKLE, C., & ROHDE, C. The sharp-interface approach for fluids with phase change: Riemann problems and ghost fluid techniques. *ESAIM Math. Model. Numer. Anal.* **41** (2007), 1089–1123. Zbl 1134.35074 MR 2377108
33. SCHULZE, S., & SHEARER, M. Undercompressive shocks for a system of hyperbolic conservation laws with cubic nonlinearity. *J. Math. Anal. Appl.* **229** (1999), 344–362. Zbl 0930.35106 MR 1664281
34. SHEARER, M., & YANG, Y. The Riemann problem for the p-system of conservation laws of mixed type with a cubic nonlinearity. *Proc. A Roy. Soc. Edinburgh Sect. A* **125** (1995), 675–699. Zbl 0843.35064 MR 1357378
35. SLEMROD, M. Admissibility criteria for propagating phase boundaries in a van der Waals fluid. *Arch. Ration. Mech. Anal.* **81** (1983), 301–315. Zbl 0505.76082 MR 0683192
36. SLEMROD, M. A limiting viscosity approach to the Riemann problem for materials exhibiting change of phase. *Arch. Ration. Mech. Anal.* **105** (1989), 327–365. Zbl 0701.35101 MR 0973246
37. TRUSKINOVSKY, L. Dynamics of non-equilibrium phase boundaries in a heat conducting nonlinear elastic medium. *J. Appl. Math. Mech.* **51** (1987), 777–784. MR 0988048
38. TRUSKINOVSKY, L. Kinks versus shocks. *Shock Induced Transitions and Phase Structures in General Media*, R. Fosdick et al. (eds.), IMA Vol. Math. Appl. 52, Springer, New York (1993), 185–229.